View metadata, citation and similar papers at core.ac.uk
brought to you by CORE
provided by CiteSeerX

Journal of Shellfish Research, Vol. 31, No. 2, 515–526, 2012.

MINERAL FINE STRUCTURE OF THE AMERICAN LOBSTER CUTICLE

JOSEPH G. KUNKEL,[1]* WOLFRAM NAGEL[2] AND MICHAEL J. JERCINOVIC[3]
[1]*Biology Department, University of Massachusetts, Amherst, MA 01003;* [2]*Physiology Institute, Ludwig-Maximillian University, D-80802, Munich, Germany;* [3]*Geoscience Department, University of Massachusetts, Amherst, MA 01003*

ABSTRACT A major role of lobster integument is protection from microbes. Calcite and amorphous calcium carbonate are the most abundant and most acid vulnerable of the cuticle minerals. We propose that calcite is invested in neutralizing an acidifying environment modulated by the epicuticle. A minor cuticle component is carbonate apatite (CAP), proposed to play critical roles in the integument's structural protective function. The CAP of lobster exhibits a flexible composition; its least soluble forms line the cuticular canals most exposed to the environment. A trabecular CAP structure illustrates efficient use of a sparse phosphate resource, cooperating in the hardness of the inner exocuticle. A schematic model of the cuticle emphasizes structural and chemical diversity. A thin outer calcite layer provides a dense microbial barrier that dissolves slowly through the epicuticle, providing an external, alkaline, unstirred layer that would be inhibitory to bacterial movement and metabolism. Injury to the epicuticle covering this mineralized surface unleashes an immediate efflux of carbonate, accentuating the normal alkalinity of an antimicrobial unstirred layer. The trabecular CAP inner exocuticle provides rigidity to prevent bending and cracking of the calcite outer exocuticle. The combined mineral fine structure of lobster cuticle supports antimicrobial function as well as plays a structural protective role.

KEY WORDS: American lobster, *Homarus americanus*, calcite, carbonate–apatite, bone, electron microprobe, ion flux, scanning ion electrode technique, SIET, unstirred layer, epizootic shell disease

INTRODUCTION

Arthropod cuticle is a classic object of study by paleontologists, morphologists, cytologists, physiologists, and biochemists (Dennell 1947, Richards 1951, Roer & Dillaman 1984, Willis 1999, Locke 2001, Havemann et al. 2008). More recently, materials scientists have viewed crustacean cuticle as an example of a time-tested natural composite material (Raabe et al. 2005). The organic polymer nature of the layered cuticle has been described as a twisted plywood pattern (Bouligand 1972, Bouligand 1986), and Nikolov et al. (2010) have computed general cuticular properties using a hierarchical averaging method. The mineral contribution to this composite, although measured (Lowenstam 1981, Boßelmann et al. 2007), has not been characterized in terms of its fine structural location; and the importance of any mineral other than calcium carbonate has been diminished. But this detail in crustaceans is now yielding to microchemical and physical measurements (Hild et al. 2009, Tao et al. 2009, Seidl et al. 2011). It is clear that crustaceans combine minerals with organic polymers in their exoskeleton to create an effective durable protective covering for a taxonomic group that has survived hundreds of millions of years, invading salt- and freshwater as well as land. The variety of cuticle composites available to be studied is drawn from among 15,000 extant species of decapods worldwide, with a species discovery curve far from flattening out (Martin et al. 2009). Arguments exist about the relative importance of carbonate and phosphatic minerals in the evolution of decapod cuticle structure with controversy over how one could switch between the two (Vega et al. 2005, Buckeridge & Newman 2006).

We show here for the American lobster, *Homarus americanus* H. Milne-Edwards, 1837, that the 3 minerals calcite, amorphous calcium carbonate (ACC), and carbonate–apatite (CAP), coexist alongside each other in discrete domains of cuticle. The freshwater and ocean environments in which the mineralized cuticle composite material needs to survive has recently changed relatively rapidly on an evolutionary timescale as a result of anthropogenic pressures (Turley et al. 2007, Ries et al. 2009), and we need to evaluate the properties of these vital skeletal structures in the light of these changes and extrapolate to the future. To accomplish this, we develop a structural–chemical model of how the American lobster cuticle is designed and behaves at macro-to-micro resolution. We also use the shell of the Atlantic jackknife razor clam, *Ensis directus* Conrad, 1843, as a simpler case in which calcium carbonate dominates, but is also covered with a superficial covering, the periostracum (Checa 2000).

MATERIALS AND METHODS

Lobsters were obtained from several locations. Lobsters with and without clinical signs of epizootic shell disease (ESD) were obtained in 2004 in shell-disease-prevalent areas from trawls by the NOAA Ship *Albatross IV* at the mouth of Narragansett Bay, RI, as well as in canyons at the edge of the continental shelf directly south of Narragansett Bay. Lobsters with signs of impoundment shell disease (ISD) were obtained May 2008 from the Maine State Aquarium at Booth Bay Harbor. Lobsters from outside the reported range of ESD were obtained June 2007 or 2008 from the State of Maine Ventless Trap Program from Casco Bay, ME, to the Isle of Shoals, NH. An equal number of lobsters with and without signs of ESD were obtained in 2008 and 2009 from Narragansett Bay, coordinates 41.5073° N and 71.3463° W.

Lobsters obtained in Maine were maintained until used in running 15°C fresh seawater at the University of New England Marine Science Center or in recirculating 15°C artificial seawater at University of Massachusetts at Amherst (UMass Amherst). Rhode Island lobsters were maintained until use in recirculating 15°C artificial seawater at UMass Amherst. Lobsters were fed daily with frozen scallop muscle *ad libitum* for 30 min. Uneaten scallop was removed.

*Corresponding author. E-mail: joe@bio.umass.edu
DOI: 10.2983/035.031.0211

Shells of the razor clam were obtained from Pine Point Beach, Scarborough, ME, shortly before use.

To study mineralization of the shell, we treated the cuticle as a moist geological specimen (Kunkel et al. 2005b). Excised, small, cuticle squares were plunge-frozen in liquid-nitrogen-cooled propane; the frozen water was then substituted with liquid-nitrogen-chilled acetone, and the pieces were brought slowly to room temperature. The cuticle was embedded in Epo-Thin Resin (Buehler). The plastic-embedded cuticle specimen was ground and polished with graded carborundum and diamond abrasive (METADI SUPREME, 6–0.25μm) suspended in polishing oil on TRIDENT polishing cloths to prevent movement of any water-soluble components (Kunkel et al. 2005b). The specimens were examined in a Cameca Ultrachron Electron Microprobe or in a Cameca SX-50 Electron Microprobe to provide electron probe microanalysis (EPMA). Using this method, a fine electron beam is scanned across a specimen surface creating at each pixel an X-ray backscatter, with a theoretical resolution of about 1 μm, which is characteristic of elements present at that location. The electron backscatter is monitored as a measure of the total density of solids at that location. The Cameca Ultrachron provides high-resolution raster images at approximately 0.33-μm resolution for up to 5 elements simultaneously. The Cameca SX-50 provided linear transects of surfaces for a chosen list of elements—Na (sodium), K (potassium), P (phosphorus), Ca (calcium), Mg (magnesium), Sr (strontium), Ba (barium), Mn (manganese), Fe (iron), Cl (chlorine), and F (fluorine)—with approximately 1-μm resolution.

Data from the EPMA instruments were exported to text files that were explored and analyzed using purpose-written R-scripts (R Development Core Team 2011) available by request. Each pixel of a the raster image from the Cameca Ultrachron has an associated data record with a column and row parameter from the m-row by n-column pixel image, and 4 columns of X-ray backscatter-determined molar composition values, typically a Ca determination, a P determination, and 2 other element determinations. In typical instances, p-by-q subregion composition data, consisting of the p × q-by-4 matrix of pixel compositions, were subjected to principal component analysis, using the R svd base library function.

Molar composition data from the Cameca SX-50 multiple linear transects of cuticle at 4-μm intervals was analyzed, and average compositional transects of regions were plotted using the lowess smoothing function in R (R Development Core Team 2011).

A general approach was to apply characterization of mineral deposits in the cuticle of multiple lobster cuticle samples from lobsters with and without lesions from shell-disease areas and lobsters from nonshell-disease-prevalent areas. We concentrated mainly on areas of healthy cuticle in our quantitative analysis, but examined apparently healthy cuticle adjacent to lesions in a number of shell-disease lobsters to determine whether early signs or stages of shell disease could be discriminated.

Ionic flux from the cuticle is measured using the scanning ion selective electrode technique (SIET) (Kunkel et al. 2005a). To measure flux emanating *in situ* from living cuticle a form-fit Tygon Tubing observational arena was glued to the cephalothorax of lobsters using Krazy-Glue Gel (Fig. 2). A Teflon nut was also glued to the cephalothorax to provide a basis for attaching a stereotactic holding device constructed from Newport clamps, rails, and posts to maintain the lobster immobile, enabling electrodes to be brought within 100 μm of the live cuticle surface for flux measurements (Fig. 2B). A minimal artificial seawater was formulated that included only the ions Na, K, Cl, Ca, and Mg in close to normal amounts compared with natural seawater (469 mM NaCl, 10 mM KCl, 10 mM $CaCl_2$, 50 mM $MgCl_2$, 2 mM $NaHCO_3$) buffered to pH 7.8–8.2 with 1 mM bis-tris-propane. This formula was selectively altered experimentally as noted, and served as the medium for measuring ionic flux to and from the cuticle surface. Both the lobster-holding chamber buffer and the observational arena buffer were cooled continuously to 15°C using a purpose-built Peltier cooling system. Measurements of flux simultaneously with 2 SIET electrodes, Ca^{2+} and H^+, held in a Dual Probe Holder (Biomedizinische Geräte, Germering, Germany) were made under ASET software control (ScienceWares, Falmouth, MA) using dual-SIET amplifiers and motion control electronics (Applicable Electronics, Forestdale, MA). The scanning polarographic electrode technique (SPET) was used to measure the oxygen flux into tissue. Platinum/iridium electrodes (PI2.5cm0036.0A10) were purchased from MicroProbes for Life Science. Data from the ASET program was exported to text files that were analyzed directly using purpose-written R-scripts (R Development Core Team 2011).

Birefringence of cuticle was examined and recorded using crossed polarizers in a Leitz Ortholux polarizing microscope using

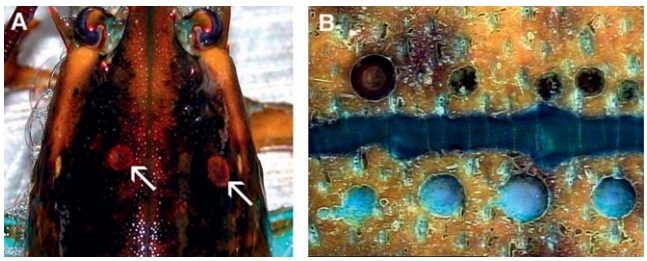

Figure 1. Natural and artificial lobster shell lesions. (A) American lobster, *Homarus americanus*, with very mild epizootic shell disease lesions. Two circular lesions are indicated by arrows. (B) Nine artificial lesions imposed on a live lobster carapace using a drill press serve as models of the lesion process. The flux of ions derived from the dissolving shell is followed by measuring differential concentrations over short distances with the specific ion electrode technique. The lesions in (B) are separated by the mid dorsal suture. The 5 upper, more melanized, lesions were produced 1 mo earlier than the bottom 4 lesions.

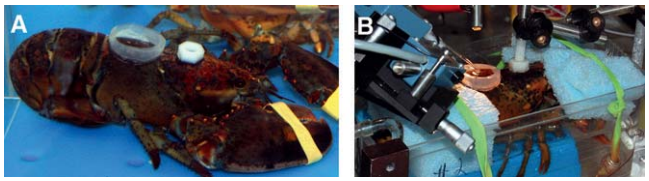

Figure 2. A lobster with a Tygon observation chamber enclosing the carapace cuticle and a Teflon-nut glued to adjacent carapace. (A) The observation chamber encloses a region of cuticle with a lesion and holds a measured amount of minimal artificial seawater. (B) This same lobster is studied with dual specific ion electrode technique probes for proton and calcium flux. The large chamber in (B) holding the lobster is temperature regulated with Peltier–cooled artificial seawater, which allows the lobster to be probed for hours and reserved afterward for probing on succeeding days. In this way, the progression of shell lesions can be followed over days or months. The objective is to identify candidate early lesions and to extrapolate back to the origin of a lesion.

reflecting optics. Artificial lesions of lobster and mollusc shells were created with a Microlux Variable Speed Drill Press (MicroMark) with a digital depth finder and 3/32-in. microball-mill drill bits.

RESULTS

In typical intermolt cuticle of a shell with no lesions we see (1) a dense, variable-thickness birefringent crystalline calcite layer as the outermost layer of the exocuticle (Figs. 3 and 4); (2) a nonbirefringent CAP lining of dermal gland and neurite canals (Figs. 4 and 5); and (3) a nonbirefringent CAP trabecular region in the inner portion of the exocuticle that corresponds to the hardness layer (Fig. 4A, B). The chemical properties of these 3 features are based on EPMA compositions of intermolt lobster cuticle seen in Figures 4 and 5, each of which illustrates different aspects of Ca and P mineral distribution in the exocuticle of the intermolt lobster. Figure 4A shows a dermal gland canal that has a canal lining of relatively low Ca:P ratio, which is typical of canals close to the surface of the cuticle. The lower limit of that ratio for CAPs is 1.67, which is the Ca:P ratio of apatite itself in which none of the phosphates are replaced with carbonates (Table 1). A cross-section of another canal seen in Figure 5 illustrates a dermal gland canal that has a canal wall with 2 regions of distinct Ca:P ratios as seen from pixel color mapping in Figure 5C and pixel Ca:P plots in Figure 5D. The 2 regions of apatite can be seen as an environment-side layer (i.e., the canal luminal layer) where Ca:P is 2, whereas the inside (cuticle matrix side) has a Ca:P of 3.51. This pattern is shown in our model to be consistent with the growth of the canal wall from the cuticle matrix side. The calcite versus CAP signals can be differentiated using principal component analysis of the composition variation among pixels. In the outlined subregion of Figure 5A, the raw pixel density data for Ca and P for a 101-by-101-pixel subregion of the image are shown in the upper panels of Figure 5C. The first principal component, PC1, explains 88.8% of the compositional variability and points efficiently to high-Ca- but low-P-content pixels that are all in the calcite layer and are discriminated by the upper PC1 values located as orange in Figure 5C (PC1 right panel) and in Figure 5D. PC2 similarly explains 9.7% of mineral variability and identifies CAP located as 2 levels of blue and green in Figure 5C (PC2 left panel), designated as wall in the right panel, and those Ca and *P* values plotted as purple in Figure 5D. The 2 ratios of Ca:P are also seen as distinctly aligned pixels with slope ratios of 2 and 3.51, respectively, in Figure 5D. Both of these ratios represent typical CAP ratios of Ca to P as seen in Table 1. A Ca:P of 2 represents CAP with a composition $Ca_{10}(PO_4)_5(CO_3)(OH)_3 \bullet H_2O$, one of the highest phosphate contents exhibited by bone that is CAP. Comparing healthy with diseased cuticle is rather simple. Lesions contain no minerals.

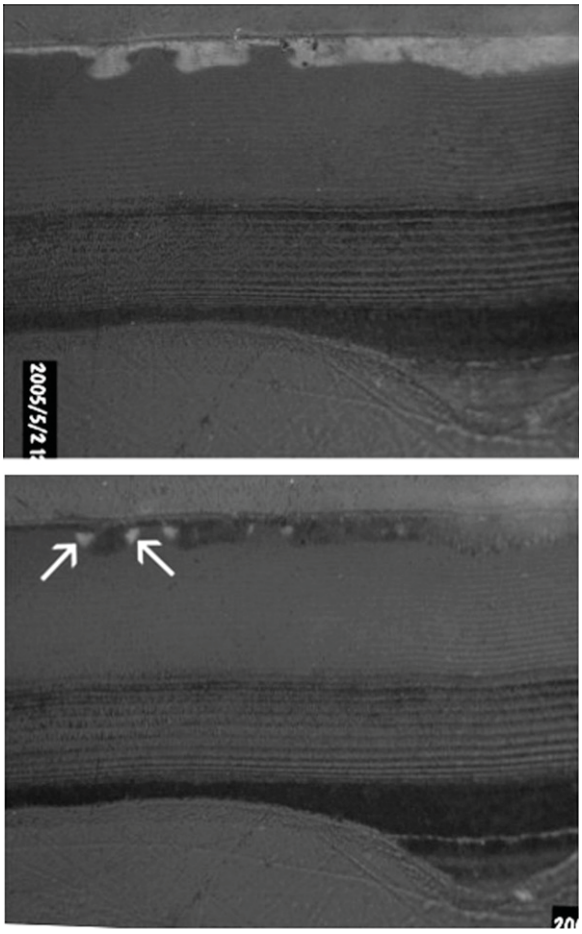

Figure 3. Birefringent calcite of healthy lobster cuticle follows surface sculpturing. Top and bottom image are same view with analyzer rotated 90°. Arrows show complementary birefringence of calcite layer on 90° rotation of analyzer.

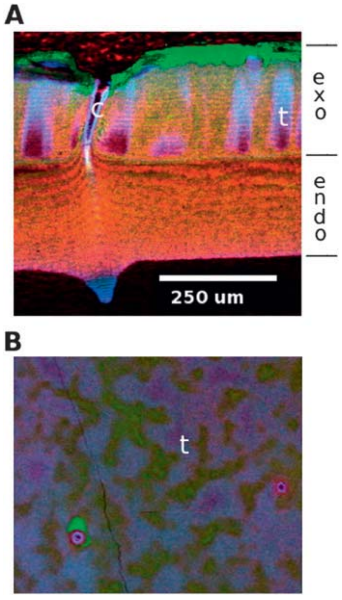

Figure 4. Lobster calcite and CAP structures interpreted as false color from 3 EMP of Ca (green), P (blue), and Cl (red) content. (A) Intermolt cuticle cross-section parallel to neurite canal (c) path showing a Ca:P composition canal wall. A thin green calcite layer colored by Ca alone. A blue nipple area at the cuticle-epidermis interface has Ca:P of 3.5. The exocuticle trabeculae (t) have Ca:P of 7. (B) A tangentially polished section of intermolt exocuticle just under the calcite layer shows Ca (green) intrusions of calcite, P (blue), and Cl (red). Purplish trabeculae (t) with Ca:P of 7 are separated by fields of amorphous calcium carbonate seen as greenish because it combines Ca with Cl. Deeper red areas indicate Cl-rich spaces surrounding the dermal and neurite canals from the background cuticle layers.

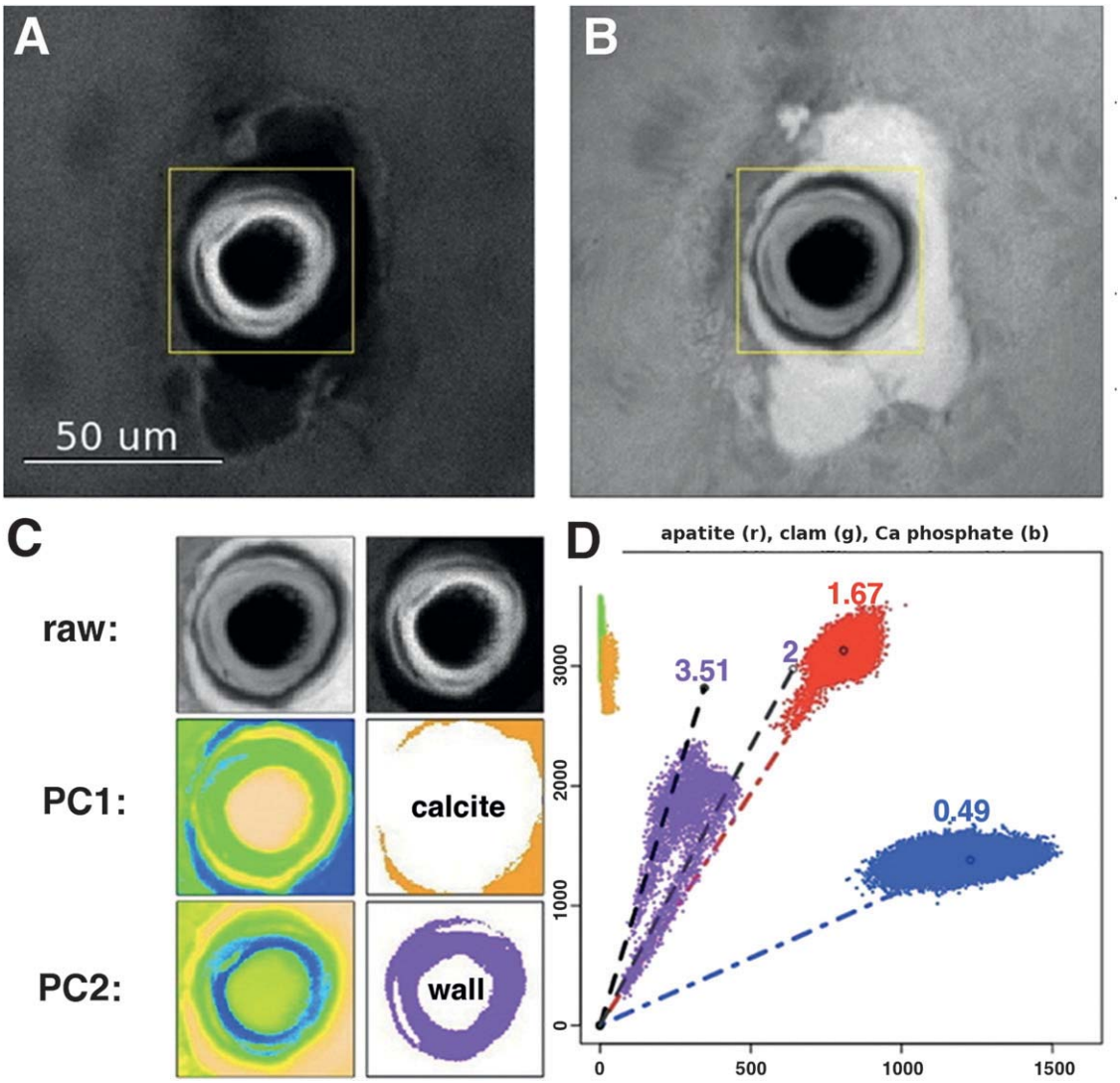

Figure 5. Tangential polished cuticle surface showing organule canal sectioned perpendicular to its long axis illustrating a calcite collar devoid of phosphate and CAP lining of the canal. (A) Phosphorous (Kα) X-ray map. (B) Calcium (Kα) X-ray map. Note the gap between the canal wall and the calcite socket. (C) Rows top to bottom—raw: selected areas of Ca, P. PC 1: Calcite PC used to choose calcite pixels. PC 2: Wall PC used to choose wall pixels. (D) Calcite and Wall pixel Ca and P contents are plotted. Slopes extrapolated through zero show the Ca:P ratios relative to clam calcite (green, no P), HAP (red, Ca:P = 1.67), and monocalcium phosphate (blue, Ca:P = 0.49). The brightness of images (A), (B), and (C-raw) scales linearly with X-ray intensity, and therefore approximately with concentrations, which are plotted to produce ratios in (D). A 50-μm calibration bar is seen in (A).

The mineral image of a lesion shows an abrupt change from mineral to otherwise healthy surrounding mineralized cuticle.

We find that the outermost mineral surface of the lobster intermolt cuticle consists mainly of a smooth dense layer of calcite (Fig. 4A) that has a calcium Kα intensity close to mollusc shell, which is 95–98% $CaCO_3$ (green pixels in Fig. 5D). This birefringent outer layer of mainly calcite appears continuous, but is punctuated at regular, but widely spread intervals by simple dermal glands with single CAP-lined canal openings, and interspersed with compound organules (Lawrence 1966) that combine sensory bristles with accompanying dermal glands (Fig. 6).

A single organule canal or bristle cell secretes a canal cuticle surrounding a narrow canal that allows an environmental outlet for secretion from an organule gland cell or forms a protective sheath around neurites innervating sensory organules, such as mechano- or chemosensory bristles at the surface of the cuticle, as seen in Figure 4A. The canal lumen in the bristle or gland canal is continuous with the outside environment and could represent a path of attack by microbes on the lumen side of the canal wall. In all arthropods, these canal passages are for carrying secretions to the cuticle surface or for protecting sensory neurites traveling through the cuticle to a sensory ending at a bristle tip. The canals have been shown in other arthropods to be lined with an epicuticle similar in structure to the epicuticle of the general surface cuticle (Kunkel 1975). The lobster cuticle has canals with an average 16-μm surface opening (range, 7–30 μm), leading into 400–1,000-μm-long canals that seem to maintain the original opening size and into which bacteria could invade and form colonies. Such canal–bacterial colonies could build up substantial populations and establish significant local focused acid gradients, potentially damaging to a calcium carbonate-based cuticle. How do the 2 distinct surfaces—the outer cuticle and the canal

TABLE 1.

Calcium phosphate and carbonate apatite formulas and Ca-to-P ratios after a general formula from Santos and Gonzalez-Diaz (1977).

x	*u*	*z*	Compound	$Ca_{10-x+u}(PO_4)_{6-x}(CO_3)_x(OH)_{2-x+2u} \bullet zH_2O$	Ca:P	Ca/P
		1	Monocalcium phosphate	$Ca(H_2PO_4)_2 \bullet H_2O$	1:2	0.5
0	0	1	Hydroxyapatite	$Ca_{10}(PO_4)_6 \ldots (OH)_2 \bullet H_2O$	10:6	1.67
1	1	1	Carbonate apatite-2	$Ca_{10}(PO_4)_5 CO_3 (OH)_3 \bullet H_2O$	2:1	2.0
2	1	1	Carbonate apatite-2.25	$Ca_9(PO_4)_4(CO_3)_2(OH)_2 \bullet H_2O$	9:4	2.25
3	1	1	Carbonate apatite-2.67	$Ca_8(PO_4)_3(CO_3)_3 OH \bullet H_2O$	8:3	2.67
4	1	1	Carbonate apatite-3.5	$Ca_7(PO_4)_2(CO_3)_4 \bullet H_2O$	7:2	3.5
4	2	1	Carbonate apatite-4	$Ca_8(PO_4)_2(CO_3)_4(OH)_2 \bullet H_2O$	8:2	4.0
4	3	1	Carbonate apatite-4.5	$Ca_9(PO_4)_2(CO_3)_4(OH)_4 \bullet H_2O$	9:2	4.5
5	2	1	Carbonate apatite-7	$Ca_7 PO_4 (CO_3)_5 OH \bullet H_2O$	7:1	7.0

In the formula, the proportion of phosphates replaced by carbonates plus hydroxyls varies, as well as the number of calciums and balancing hydroxyls to produce a balanced formula. In reality, chlorides and fluorides may replace hydroxyls to provide bone with modified properties such as with fluoride-based hardening of bone (Mirtchi et al. 1991).

lining—perform when confronted with bacterial colonization in the lobster?

When observed using EPMA (Figs. 3, 4A, and 5), the calcium Kα intensity of the calcite layer is close to that of crystalline calcite of mollusc shell, used as a standard (Fig. 5D). The calcite layer thus has limited space remaining for organic polymer. When this thin calcite layer has a small artificial lesion drilled into it, no prophenoloxidase (PPO) is activated. Only when the calcite layer is breached and the inner exocuticle is exposed, is PPO activated. The crystalline calcite layer can be observed in polarized light as a uniformly birefringent layer that can turn corners, indicating its controlled orientation (Fig. 3, arrows), most likely deposited along polymer fibrils or bundles laid down by the formative general epidermal and derived organule cells (Lawrence 1966, Merritt 2007). Consistent with this, the numerous pore canal filaments represent microvillar extensions of the epidermal cells that course through the physiologically living endo- and exocuticle, but are excluded from the calcite layer (seen in unshared AFM figures). The remnant spaces, formerly occupied by live filaments, are surrounded by organic and mineral layering observed with EPMA and by AFM, but essentially end at the inner surface of the calcite layer. The crystalline density, seen in Figures 4 and 5, of the calcite layer does not afford a spatial avenue for pore canal filaments or microbial attack in the dimensions of typical bacteria unless the density was first compromised by erosion or cracking. The calcite layer also extends down like a collar along the canal wall exterior at the organule canal intersection, seen in cross-section in Figure 4A, and in tangential section in Figure 4B (as red-coded Cl) and Figure 5B. The canal wall abuts the calcite collar closely, leaving a relatively small space between the mineral faces, particularly visible in the calcium image (Fig. 5B). The calcite layer and its boundary with the apatite tubes might allow access into the cuticle by microbes down to the typical size of a bacterium (0.2–2 μm), and we may need to know the tolerances of this space under stress as predicted by our model. We do not know the organic composition of that thin space, but when other ions are analyzed via EPMA, the space is seen to contain Cl and K, which indicate it is or was a soluble-ion-containing cellular compartment.

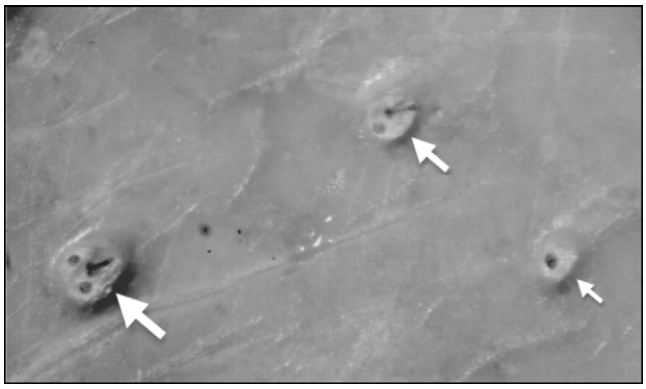

Figure 6. Primary, secondary, and tertiary organule cuticle structures on the dorsal carapace of an intermolt lobster. Three size and complexity levels for organules are presented and pointed to by arrows that increase in size. The first level is a simple gland tube opening, the second combines a bristle and a gland opening, and the third level has more organule components.

The flat surface of the general cuticle surface does not encourage the buildup of a pH gradient from a bacterial colony growing on an open surface. This is because protons in water as hydronium ions have an anomalous 12-times faster diffusion than their diameter predicts (Kunkel et al. 2001). This is the physical reason that a calcite surface is a sufficient material to create a physical barrier to microbial attack; protons created by a point source group of bacteria disperse rapidly and do not accumulate enough titer to do damage to the calcite. In addition, the calcite layer of the cuticle is also covered by a waxy epicuticle, which is efficient protection from bacterial attack for another reason: During the slow solubilization of calcite,

$$CaCO_3 \Leftrightarrow Ca^2 + CO_3^{-2}, \quad (1)$$

through the epicuticle into the ocean water, carbonate and Ca ions are released. The carbonate takes a proton from water,

$$H_2O + CO_3^{-2} \Leftrightarrow HCO_3^{-1} + OH^{-1}, \quad (2)$$

becoming bicarbonate and releasing a hydroxyl, which is stabilized at the ambient pH and thus results in a widely based alkaline zone in an unstirred layer (Pohl et al. 1998) adjacent to the cuticle. The unstirred layer gradient properties are a result of the speed with which diffusion of an ion establishes a nearby high pH gradient, despite competing bulk flow of nearby ocean

water that eventually and undoubtedly affects the gradient depletion. The high standing pH gradient, approaching pH 9 nearest the cuticle surface, is dispersed as it declines into the bulk of the adjacent seawater (pH 7.8–8.2), but the thin, relatively more alkaline, aqueous surface unstirred layer remains on any calcium carbonate-based shell as an antibiotic to bacterial motility, metabolism, and growth (Palmer et al. 1997, Bombelli & Wright 2006). It also neutralizes any microbial acidic action on shellfish exoskeletons, which we here propose as a novel general immune mechanism. Calcite itself would not be an effective material choice as a lining of the cuticular organule canals because in the enclosed small diameter (but extended length) of a gland or neurite canal, proton gradients could be established by bacteria that could dissolve a calcite lining easily. Rather, the organule's canal is lined fortuitously by the phosphatic mineral CAP of moderately high density that is more acid resistant than calcite. Chemical analysis of this layer by EPMA demonstrates (Figs. 4 and 5) that in Ca:P ratio it conforms to the flexible composition of CAPs (Table 1) (Santos & Gonzalez-Diaz 1977, Wopenka & Pasteris 2005), being relatively resistant to acid solubilization. The only other calcium phosphate that could theoretically apply is tetracalcium phosphate, a mineral not described in living tissues (Dorozhkin & Epple 2002). Either mineral would provide the ratio of Ca:P of approximately 2, which is observed in some neurite- and gland-canal walls. These most exposed canal linings have close to a 2:1 Ca:P ratio in CAP composition, making it least sensitive to acid attack (Baig et al. 1999). Interestingly, the phosphatic deposits as seen in 2 locations in lobster cuticle exhibit several of the generally accepted formulations of cap (Table 1) that have flexible Ca:P ratios that can include 2:1, 2.25:1, 2.67:1, 3.5:1, 4:1, and 7:1, which are all discretely observed (Figs. 4 and 5) in canal tubes having Ca:P ratios predicted by the CAP formula of Table 1. The discreteness of the CAP formulations is often emphasized by finding 2 Ca:P ratios in a single cross-section (Fig. 5A, D). The variety of Ca:P ratios exhibited by lobster cuticle is explored more extensively elsewhere (Kunkel & Jercinovic 2012).

The composition of the calcite inner exocuticle and endocuticle layers were studied in greater detail using 12 quantitative transects of lobster intermolt cuticle using the SX-50 electron microprobe. Care was taken to include transects through trabecular as well as nontrabecular regions of the cuticle, which changed the chemical profiles mainly in the inner exocuticle, which the trabeculae populate. With the SX-50 electron microprobe we were able to measure the content of the other group 2 alkaline earth metals, providing additional detail on the regional heterogeneity of the lobster cuticle. Figure 7 shows the relative titers of Mg, Ca, Sr, Mn, and Ba. Of particular note is the precipitous decline in Mg, Sr, Mn, and Ba, together in the calcite layer toward the surface of the cuticle. This may represent a clue to the role of the minor divalent ions in the calcite layer function. Although Mg is known for its hardening properties in calcite composition, it is also known for its higher solubility and concentration in the ocean. A more rapid dissolution of $MgCO_3$ in the surface-oriented calcite could provide extra protection from microbes via raising the unstirred zone's pH.

Our application of SIET and SPET to study the flux of ions and oxygen in relation to the cuticle and early-stage lesions was frustrated by very few examples of early lesions to which we could apply our measurement of Ca and proton flux. However, from the few such lobsters, that in Figure 2A being one of them, it was evident that there was a slow flux outward of Ca^{2+} and inward of H^+ from lobster cuticle not showing signs of shell disease, and a substantial increase of that flux over lesions. This observation rejected immediately our earlier naive hypothesis that we should detect early latent or developing lesions from the secretion of protons by a microbial film or colony at the site of a future lesion. Ionic flux from the lobster cuticle with or without signs of shell disease is dominated by calcium carbonate dissolution from the

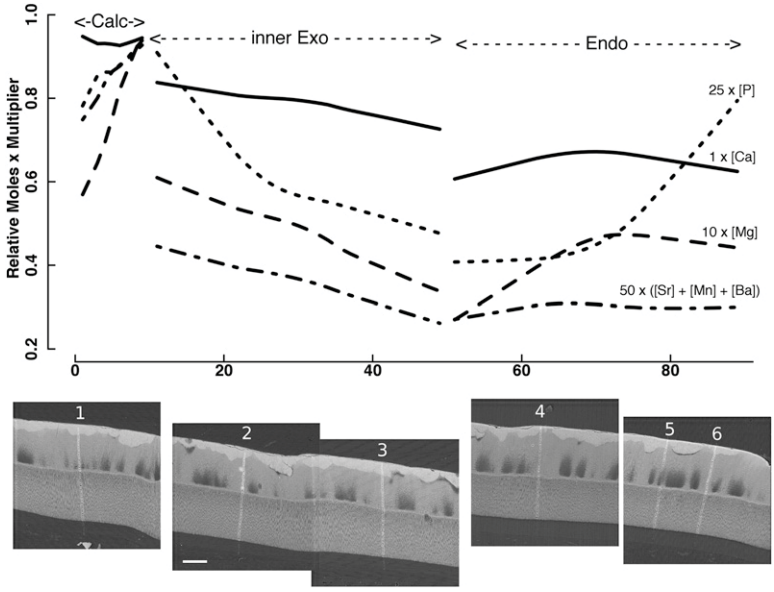

Figure 7. Divalent cation (Mg, Ca, [Sr + Mn + Ba] and P) molar content of the 3 distinct lobster intermolt cuticle layers: calcite (Calc), inner exocuticle (inner Exo), and endocuticle (Endo) were measure by EPMA. The average relative molar composition is calculated from 6 100-point transects of the approximately 400-μm thick cuticles. The lowess smoothed averages are plotted against their position in the layers. The relative molar contents are normalized at the inner edge of the calcite layer, using the listed multiplier, to allow easier comparison. The paths of the 6t transects are shown in 5 electron backscatter images. A 100-μm calibration bar is presented with the image of scan 2.

superficial calcite layer of the exocuticle. The entire surface of the lobster carapace slowly leaches $CaCO_3$ from the calcite layer, creating a basic unstirred antimicrobial surface environment.

More productive information was obtained by our creation of graded artificial lesions such as that seen in Figure 1B. Such artificial lesions allowed us to examine numerous lobsters with different degrees of lesion reaching various levels in the cuticle, and studied at various times after lesion creation. These lesions were examined using dual Ca- and H-LIX microelectrodes simultaneously at the same location (Fig. 8). The pattern was highly reproducible. The Ca flux was the mirror opposite of the H flux. Ca^{2+} appeared to exit the lesion, and H^+ appeared to enter the lesion. This is explained by the dominant equilibrium reaction (Eq (3)) occurring at the pH of the lobster's environment combining reactions (1) and (2):

$$CaCO_3 + H_2O \Leftrightarrow Ca^{2+} + HCO_3^- + OH^- \quad (3)$$

The $CaCO_3$ dissolution reaction produces Ca^{2+} and OH^- at the surface of the cuticle, from which we measure the outward-diffusing Ca^{2+} and OH^- as outward-diffusing Ca^{2+} and inward-diffusing H^+. This opposite but approximately equal flux of Ca^{2+} and H^+ is a signature of dissolving calcite or aragonite or ACC, and would distinguish $CaCO_3$ dissolution from $CaCl_2$ dissolution, for instance, or from simple Ca^{2+} export linked to some other balanced transport.

We did not find any particularly enhanced or diminished flux of Ca^{2+} or H^+ over the organule canal openings, which indicates that they are well surrounded by calcite at the surface, as indicated in Fig. 4A. Moreover, neither the dermal gland nor the bristle organules presented an avenue of enhanced or diminished Ca^{2+} or H^+ flux, at least in their asymptomatic (apparently nonlesion) state.

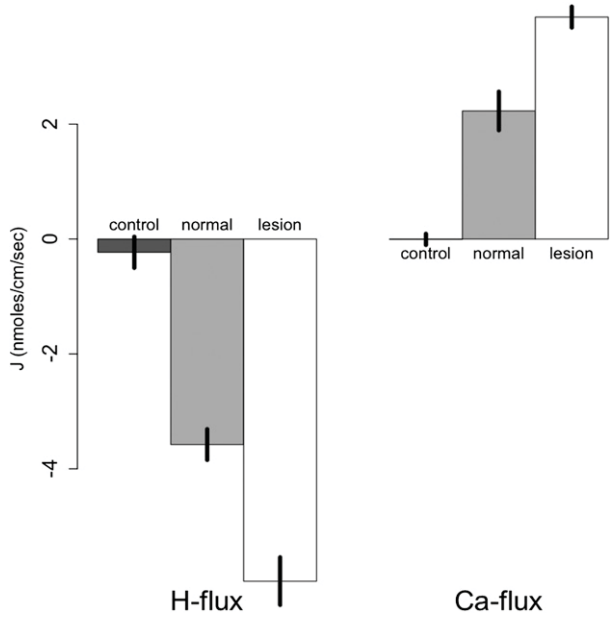

Figure 8. Ca and H flux from artificial lesions in lobster cuticle. The Ca and proton flux mirror each other above asymptomatic and artificially lesioned cuticle as predicted for a calcite source by our model (Fig. 10). Control measurements are made 2 mm above the cuticle surface. Error bars represent ±1 SEM for 10 observations.

When the calcite layer is penetrated by an artificial lesion, such as those seen in Figure 1B, a stronger linked outward flux of Ca^{2+} and H^+ is measured because the dissolution of ACC has a lower energy requirement and thus it dissolves more quickly. The design of a calcite layer underlain by an ACC layer can be seen as selectively advantageous in fighting a progressive shell disease lesion. This supplements the role that ACC has in generating calcite (Pouget et al. 2009) during the postmolt, when the calcite layer is being established. In our view, the ACC deposits between the trabeculae in the inner exocuticle and in the general endocuticle serve as a reservoir of quickly deployable calcium carbonate that can aid in responding to injury by lowering pH in the ~100-μm unstirred layer above an injury.

Using the polarographic micro oxygen electrode (SPET), the development of oxygen utilization by lesions was followed. New artificial lesions, in the first hours after formation, showed only very small oxygen flux into the lesion, indistinguishable from the surrounding nonlesioned cuticle. Artificial lesions, 24 h after being established, developed visible signs of melanization and, when tested via SPET, showed a strong inward O_2 flux, appropriate to the activation of PPO, which is apparently activated by that time.

Broadening our understanding of the phenomenon of balanced outward Ca^{2+} and inward H^+ flux that we observed first in the lobster, we have studied mollusc calcite shells that are also covered by a protective layer, the periostracum, a protein polymer layer laid down and sometimes maintained actively by the mollusc mantle tissue. This periostracum is analogous to the epicuticle of the lobster in that it protects the calcite layer. We extend the agreed-upon protective role during shell formation (Marin & Luquet 2004) by our proposal that the periostracum affords further protection from rapid dissolution during the useful life of the shell. We demonstrate that artificial lesions created in the mollusc periostracal covering release a stream of Ca^{2+} and OH^- ions similar to those we have observed emanating from our lobster artificial lesions (Fig. 9). In this instance, the ratio between the flux at the center versus the edge of the lesion over intact periostracum is 8.9 (±1.9 SE)-fold. This ~9-fold increase over a shell lesion is probably closer to an accurate measure because it is easier to get close to the inert shell surface than the live lobster cuticle surface.

Study of the mollusc and lobster cuticle artificial lesions demonstrate that the Ca and H fluxes mirror each other in direction and strength. The H flux into the lesions represents the expected flux created by the opposite flow of hydroxyls created by reaction (3), as diagrammed in Figure 6. The artificial removal of the epicuticle doubles the fluxes measured from nonlesion cuticle even as viewed at the 100-μm distance from the surface, thus demonstrating that the epicuticle serves as a modulator of calcite dissolution. The pH at the shell surface in the low-micrometer space occupied by bacterial films is likely to be close to pH 9, the pK of CO_3^{-2} reaction with water.

DISCUSSION

The 2 distinctly different forms of shell disease, ISD and ESD, attack at different points of the lobster cuticle based on substantial past histological study and experience (Smolowitz et al. 1992, Hsu & Smolowitz 2003, Tlusty et al. 2007). ISD attacks at the dermal gland canals, and ESD on the plane between dermal gland canals. This difference in point of attack allows us to create hypotheses about the progression of shell

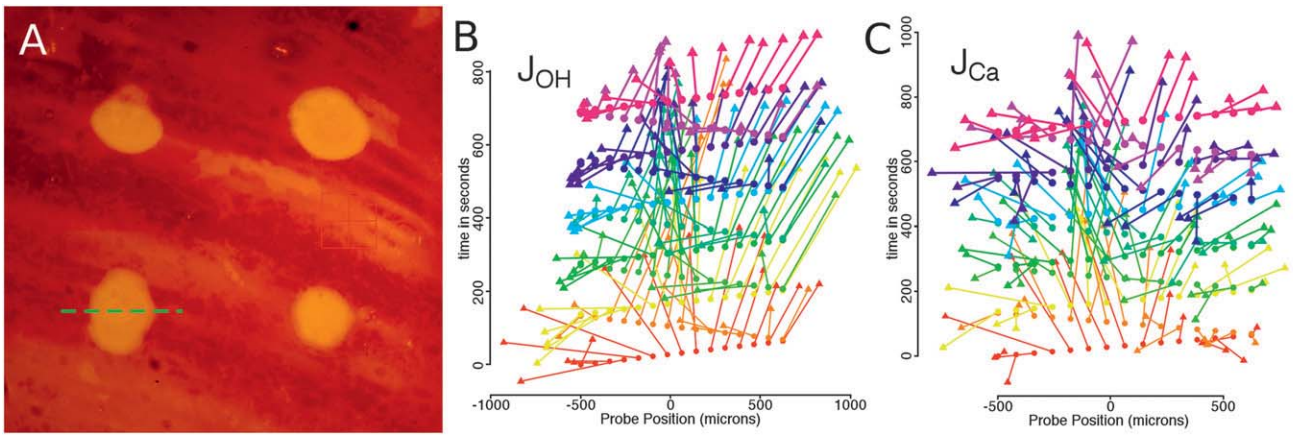

Figure 9. Ca^{2+} and H^{+} flux vectors emanating from an artificial lesion through the periostracum, protective layer, of a razor clam. (A) Image of 4 artificial lesions drilled in the surface of a shell. The dashed green line shows the 1,200-μm-long path of the dual Ca and H microelectrodes, which were scanned repeatedly across that same path measuring the flux of those 2 ions in both the x-direction parallel to the path and the z-direction perpendicular to the shell surface. (B, C) These 2-dimensional fluxes are plotted as vectors in (B) for the H flux interpreted as the complementary OH flux and (C), where the Ca flux is depicted. Time is measured in seconds from the introduction of a new artificial seawater buffer of pH 7.8, allowing the speed of establishment of the ion gradients to be followed. The earliest vectors are depicted thin and become thicker as time progresses. The origin of each vector is a filled circle whereas the apex of the vector is indicated as a triangle. The earlier fluxes are stronger because they are responding to a larger differential concentration; as the difference is moderated by dissolution, the fluxes moderate. This is an automated governor on dissolution rate associated with lesions. In the lowered pH of the benthic environment, the 10 mOsm Ca^{+2} and 2 mOsm total CO_3^{-2} represents an undersaturation for $CaCO_3$.

disease based on predictable vulnerabilities of a model we construct (Fig. 10). This model emphasizes our new interpretations of the roles of the 3 minerals that we suggest dominate the mineralized cuticle: calcite, ACC, and CAP. In pursuit of this theory, we describe how our cuticle model might provide a protective role using our focus: the minerals. Our model, based on some key exemplar physical evidence (e.g., Fig. 3–5), and physiological evidence (Figs. 8, 9) suggests a protective rationale and a structural role for each key mineral of the lobster cuticle. Each mineral and its survival benefits may have provided a selective force during the structural evolution of crustacean cuticle. We suggest that one of the most powerful forces in that evolution has been resistance to microbial attack.

The resistance to microbial attack is 3-fold. First, we posit a continuous, dense calcite layer that provides a physical barrier to microbial attack on the organic polymer layers. Second, we posit a modulating epicuticle layer that allows the calcite layer to dissolve gradually, producing an antimicrobial unstirred layer that covers the cuticle surface with a thin environment unfavorable for microbial growth. Third, we posit the use of acid-resistant CAP to line the vulnerable canals that must traverse the cuticle.

Several potentially vulnerable aspects of the dermal glands are derived from inspecting our model of the lobster cuticle. The phosphatic walls of each canal need a tight interface with the cuticle's calcite layer (Fig. 4A, B). The visible space between the 2 mineral structures seen particularly in Figures 5B and 4B is filled with the chloride anion. What are the acceptable tolerances of these spaces? There is a possibility of a failure in the phosphate or carbonate chemistry for this juncture—particularly in the crowded and altered water quality of lobster pounds and rearing facilities, after which the ISD is named. There is also ample evidence of the limiting nature of available phosphate in the North Atlantic arena (Wu et al. 2000, Zubkov et al. 2007). In the altered temperature, pH, salinity, nutrient, and microbial environment of a lobster pound or aquarium, the chemistry of cuticle formation could clearly be a source of problems. The canals and their interface with the calcite layer need to be replaced at each molt. During the molting process, existing cuticular organules are moved apart from each other during the generally isometric expansion of the cuticle surface. The expansion of the cuticle in lobsters at each molt varies, but is increased approximately 1.1-fold in linear dimensions that represent a 21% increase in cuticle area. New organules need to develop and be inserted into the widening expanses of cuticle devoid of organules. This process is described more thoroughly in Kunkel and Jercinovic (2012). The development and replacement of the canals and calcite interface may be critical vulnerabilities that need to be protected during each molt. A lowering of pH, for instance, makes the energy necessary for retrieving carbonate from bicarbonate more costly to the lobster. If the phosphatic lining of the dermal gland and neurite canals was thinner or more acid vulnerable compositionally for some reason, the ability of bacteria to access and attack the underlying chitin and protein linkages could be encouraged. In addition, an acidified seawater environment might allow a pH gradient produced by a bacterial colony to be more effective, given a lower imposed pH environment at the opening of the organule canals or incipient imperfections in the calcite layer or calcite–CAP interface. These avenues of attack can be pursued in a tightly defined chemostat arena or in a relatively simple marine life-table flow-through environment by adjusting the conditions that interact to allow the impoundment type or epizootic type of shell disease to develop.

The study of ESD with respect to our model is perhaps less straightforward. So far, it has been difficult to say exactly where in the mineral cuticle a lesion initiates, because it destroys its locus at the point of attack. How the lesions initiate in the plane between organules is not easy to envision or approach experimentally. Our model suggests several potential sources of weakness in the cuticle. During experimentation, efforts must be taken to avoid the conditions of ISD from occurring. The most likely accidental initiation

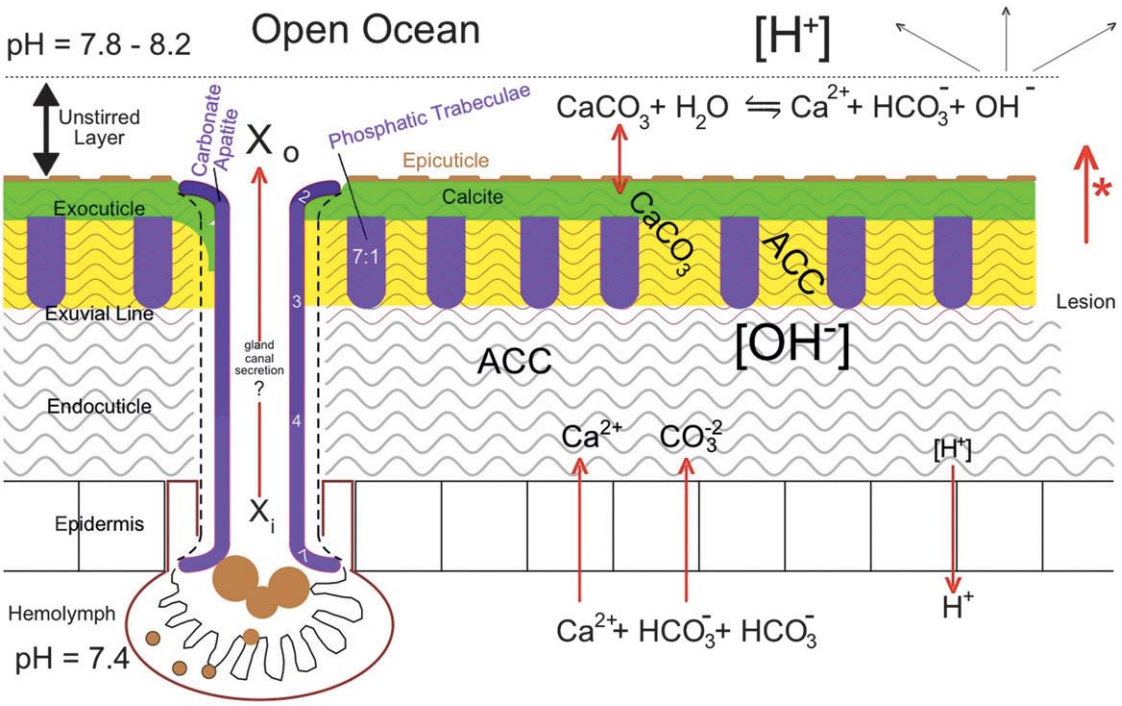

Figure 10. Schematic model of lobster cuticle and basal and apical environment including a dermal gland with graded (2:1–7:1 Ca:P) carbonate apatite-lined canal (Kunkel & Jercinovic 2012) secreting a product Xi → Xo. Phosphatic trabeculae are 7:1 Ca:P. During cuticle production, Ca^{2+} and CO_3^{-2} are imported into the cuticle space from the hemolymph side, balanced by the expulsion of a proton. At the cuticle outer surface, the epicuticle regulates a slow dissolution of the calcite layer, which produces a continuous stream of hydroxyls into the unstirred layer, raising its pH as the dissolving $CaCO_3$ combines with water. The unstirred layer is ultimately in a dynamic equilibrium with the open ocean, which is nominally at pH 8.2, but probably closer to pH 7.8 in the lobster's benthic environment. A lesion (asterisk arrow) makes more soluble amorphous calcium carbonate (ACC) available for rapid alkalinization of the superficial unstirred layer.

might be via a crack or imperfection during initiation of the calcite layer after molting. Avoiding cracks in the calcite layer that occur later during the intermolt period may depend on the proper rigidity of the underlying phosphatic trabecular layer. The evidence from light microscope sections of demineralized cuticle from early ESD lobsters (Hsu & Smolowitz 2003) suggests that when the newest lesions develop in the calcite-plane region between the organules, they produce pillars of relatively undigested cuticle. We suggest that these pillars occupy the spaces between the more acid-resistant phosphatic trabeculae of the inner exocuticle (Fig. 4A). Our work with oxygen electrodes on artificial lesions of the cuticle, described briefly earlier, suggest that until the thin, dense calcite layer is compromised, there is no response of oxygen utilization by the lesioned cuticle. Once the calcite layer is breached, the cuticular PPO is activated, oxygen starts being used, and melanin accumulates at the lesion, as seen in Figure 1B. Therefore, the first hypothetical point of attack in ESD would be an imperfect calcite layer that propagates through the least resistant regions, which would be the ACC columns between the phosphatic trabeculae. This might occur because the calcite layer was not developed properly from available ACC during the time shortly after ecdysis, during the phase that the cuticle provisionally hardens, or it could result from the attack of this layer after it had been formed imperfectly or cracked because of improper development of the more rigid underlying trabecular layer. Thus, our hypotheses on how lesions might develop depend on the structural richness of our model.

Previously, modeling from a structural engineering point of view, Nikolov et al. (2010) have computed general cuticular properties by a bottom-up hierarchical averaging method. This averaging of properties inherent in the former approach minimizes the importance of unique properties of localized specializations such as the epi-, exo-, and endocuticle layers of the cuticle as well as the overdispersed organules, the glands and neural canals that populate the cuticle surface. Our top-down modeling approach was to focus quantitatively on the visible localized structures and properties that we then integrated into our structurally diverse model, with additional emphasis on paying attention to general surface properties most important in defense against external microbial attack.

The diseases affecting the cuticular structure of the American lobster could provide clues to how a more realistic lobster cuticle composite design is vulnerable, and how the vulnerabilities might be attacked and defended. Our schematic model of mineralized American lobster cuticle provides arguments for how the cuticle defends its owner against chemical and microbial attacks such as seen in lobster ISD (Smolowitz et al. 1992) and ESD (Fig. 1A) (Hsu & Smolowitz 2003). Future materials science hierarchical averaging approaches to constructing a less uniform composite model of the lobster cuticle may benefit from incorporating the focal properties that we have identified. For instance, we observe that the surface calcite layer is enriched with Mg^{2+}. The early dissolution of $MgCO_3$ from the surface of the calcite layer, leaving its environmental face lower in Mg as we observe it, may provide an early, postmolt-intense alkalinization of the unstirred layer that provides additional bacterial resistance. Such details may be key in the functional strategy of the cuticle's composite structure during the vulnerable days after ecdysis.

We discuss the 4 structural details we have identified: CAP trabeculae, CAP canals, the surface calcite layer and ACC.

Heterogeneity in structure such as our observed spongy, bonelike trabecular structure brings up the possibility of its responsibility for the slow, progressive hardening of lobster carapace cuticle as described by Waddy et al. (1995). Based on our mineralization maps and our model, and the hardness tests of Raabe et al. (2005), it seems that the hardness would not coincide with the outer calcite density. In their progressive indentation tests (Raabe et al. 2005), the outermost layer, corresponding to the calcite layer of our studies in thickness, is a moderately soft outer layer. That layer would need to be established relatively quickly after molting for self-protective reasons based on our model. The slower development of hardness would correspond to the zone of the phosphatic trabeculae (i.e., the inner exocuticle), which would develop more slowly depending on available phosphorous. Living in the northern Atlantic P-poor environment (Wu et al. 2000, Zubkov et al. 2007), the American lobster may have developed a strategy of using its limited P availability by slowing down the cuticle hardening process as we know it (Waddy et al. 1995). Our model provides an imperative for efficient phosphate investment (1) as organule canal walls protecting secretion and neurosensory communication and (2) as phosphatic trabeculae to be associated with the well-described (Waddy et al. 1995) gradual hardening of the lobster cuticle that occurs after ecdysis.

The lobster trabeculae are possibly convergent with the trabeculae of vertebrate spongy bone in ways beyond chemical structure. The dynamics of the development of the lobster trabeculae may well be based on stress. The dorsal carapace is the site of many thoracic muscle attachments, and the stress provided by those attachments could result in, or depend on, the massive hardness that develops at the dorsal lateral carapace versus the thinner lateral ventral carapace sides that cover the branchial cavity. A stress model of lobster bone development may also apply to the thickness of chelae cuticle that could be adjusted behaviorally by how the lobster uses its crusher versus cutter chelae.

ACC is found between trabeculae of the exocuticle perhaps associated with chitin and protein fibrils, as demonstrated in a marine isopod (Seidl et al. 2011). This inherently soft mineral form is similar in electron density to the ACC found in the endocuticle that is measurably the softest layer of the lobster cuticle based on the measurements of Raabe et al. (2005). This ACC may be an essential reserve of available calcium carbonate that can provide the calcium for trabecular development and also respond to cuticular injury by dissolving to form a flush of alkalinity in the unstirred layer that is an antimicrobial shield for the cuticle. This interpretation extends the role of ACC beyond being merely a precursor to crystalline calcium carbonate forms, as proposed previously (Pouget et al. 2009). Exocuticle composed of pure CAP would be a waste of scarce phosphate but also would not serve as a ready source of antimicrobial alkalinity.

The general marine environment is becoming more acidic, which may exacerbate shell diseases, particularly for shellfish that depend on calcium carbonate. Observations from nature, laboratory experiments (Orr et al. 2005), and modeling (Ridgwell & Schmidt 2010) are currently unclear in how severely the environmental changes in pH and mineral saturations impact each species' future survival. Some species with mineral deposition that is accomplished at ambient ocean calcium carbonate saturation are clearly threatened by ocean acidification. Others that deposit their minerals in a protected environment are less directly affected (Ries et al. 2009). Cuticle mineralization in decapods for Ca^{2+} and CO_3^{-2} is generally considered to be accomplished from the epidermal side of the cuticle after ecdysis (Compere et al. 1993, Wheatly 1999), buffered from the open ocean by the animal's internal milieu. Thus, it is unlikely that the modest changes in pH of the ocean will have a major effect on the ability of the lobster to produce a cuticle. However, the proper functioning of that cuticle on its outside surface, which is in nearly direct contact with the ocean, is clearly vulnerable to environmental changes. Our model cautions that simple cuticle deposition or bulk composition may not be the critical factor for the lobster. The model of the lobster cuticle provides more variables to be considered in the ability of individual lobsters to survive in their current environment, and we are cautioned to pay closer attention to the details of each species' compositional and structural mechanisms of protection in their local environments.

It is of some interest to discuss how other immune factors might interplay with the calcite-based antimicrobial function. For instance, PPO is known to be activated by injury. To what extent does PPO provide similar or additive immunity from microbial attack? Clearly PPO has a role in immune responses to lesions in cuticle for a broad selection of arthropods. In the artificial lesions created in our experiments, the melanization of the cuticle was visible by 24 h after the lesion was made through the calcite layer. The calcite dissolution response is immediate. The encapsulation of the lesion by melanization is relatively slow, based on our measurement of oxygen utilization by those lesions. No increased oxygen utilization was measureable within hours of lesion initiation. This is perhaps a result of the need for a relatively slow enzymatic activation of the PPO. After 24 h, a dramatic increase in oxygen utilization was exhibited, and one can actually see melanization product in the lesion (Fig. 1B). Clearly, the melanization has some role in stabilizing the lesion by cross-linking the cuticle proteins, and if it is a microbial lesion, the microbes may well be somewhat inhibited in further aggression in the lesion. However, the alkalinization of the unstirred layer is already a constant factor in the nonlesioned cuticle and is immediately increased dramatically after a lesion occurs. In addition, after the lesion penetrates through the epicuticle and calcite layers, the underlying ACC is yet more easily solubilized, creating a stronger alkaline flux into the unstirred layer. How effective this is and how it interacts with the PPO activation is yet to be established.

The main effect of phenoloxidase on cuticle function may indeed be proactive, occurring during the early phase of cuticle sclerotization, when the phosphatic trabeculae are developing in the region of the inner exocuticle that is being cross-linked by quinones. This critical cuticle construction process may be affected by alkylphenol pollutants experienced by the lobster that inhibit the phenoloxidase enzyme activity as explored elsewhere in this volume (Laufer et al. 2012). Our model of the cuticle affords specific structures and timing that could be affected by the enzyme malfunction.

It is clear that the normal and lesion-induced alkalinization by the calcite layer has affects on bacterial cells in general, but probably has little affect on eukaryotic microbes (Palmer et al. 1997). Therefore, other immune mechanisms must be present to defend the cuticle from nonbacterial microbes, such as fungi, that are targets of antimicrobial peptides, which have been described in decapods (Rosa & Barracco 2010) but have been more associated with more advanced breaches into the hemocoel. Last, the newly described architecture involving calcite,

ACC, and CAP in the lobster cuticle allows us to explore a new model for skeletal function in a nonvertebrate.

ACKNOWLEDGMENTS

This work was supported by a seed grant from MIT Sea Grant, by the National Marine Fisheries Service as the New England Lobster Research Initiative: Lobster Shell Disease under NOAA grant NA06NMF4720100 to the University of Rhode Island Fisheries Center, and an NSF-funded collaboration of Cameca and UMass Geosciences. The views expressed herein are those of the authors and do not necessarily reflect the views of NOAA or any of its subagencies. The U.S. government is authorized to produce and distribute reprints for government purposes, notwithstanding any copyright notation that may appear hereon.

LITERATURE CITED

Baig, A. A., J. L. Fox, R. A. Young, Z. Wang & J. Hsu. 1999. Relationships among carbonated apatite solubility, crystallite size, and microstrain parameters. *Calcif. Tissue Int*. 64:437–449.

Bombelli, E. C. & E. R. Wright. 2006. Efecto del bicarbonato de potasio sobre la calidad del tomate y acción sobre *Botrytis cinerea* en postcosecha. *Cienc. Invas. Agric*. 33:197–203. (in Spanish).

Boßelmann, F., P. Romano, H. Fabritius, D. Raabe & M. Epple. 2007. The composition of the exoskeleton of two Crustacea: the American lobster *Homarus americanus* and the edible crab *Cancer pagurus*. *Thermochim. Acta* 463:65–68.

Bouligand, Y. 1972. Twisted fibrous arrangements in biological materials and cholesteric mesophases. *Tissue Cell* 4:189–217.

Bouligand, Y. 1986. Theory of microtomy artefacts in arthropod cuticle. *Tissue Cell* 18:621–643.

Buckeridge, J. S. & W. A. Newman. 2006. A revision of the Iblidae and the stalked barnacles (Crustacea: Cirripedia: Thoracica), including new ordinal, familial and generic taxa, and two new species from New Zealand and Tasmanian waters. *Zootaxa* 1136:1–38.

Checa, A. 2000. A new model for periostracum and shell formation in Unionidae (Bivalvia, Mollusca). *Tissue Cell* 32:405–416.

Dennell, R. 1947. The occurrence and significance of phenolic hardening in the newly formed cuticle of Crustacea Decapoda. *Proc. R. Soc. Lond. B Biol. Sci*. 134:485–503.

Dorozhkin, S. V. & M. Epple. 2002. Biological and medical significance of calcium phosphates. *Angew. Chem. Int. Ed*. 41:3130–3146.

Havemann, J., U. Müller, J. Berger, H. Schwarz, M. Gerberding & B. Moussian. 2008. Cuticle differentiation in the embryo of the amphipod crustacean *Parhyale hawaiensis*. *Cell Tissue Res*. 332:359–370.

Hild, S., F. Neues, N. Znidarsic, J. Strus, M. Epple, O. Marti & A. Ziegler. 2009. Ultrastructure and mineral distribution in the tergal cuticle of the terrestrial isopod *Titanethes albus*: adaptations to a karst cave biotope. *J. Struct. Biol*. 168:426–436.

Hsu, A. C. & R. M. Smolowitz. 2003. Scanning electron microscopy investigation of epizootic lobster shell disease in *Homarus americanus*. *Biol. Bull*. 205:228–230.

Kunkel, J. G. 1975. Cockroach molting: I. Temporal organization of events during molting cycle *Blattella germanica* (L.). *Biol. Bull*. 148: 259–273.

Kunkel, J. G., S. Cordeiro, Y. Xu, A. M. Shipley & J. A. Feijo. 2005a. The use of non-invasive ion-selective microelectrode techniques for the study of plant development. In: A. G. Volkov, editor. Plant electrophysiology: theory and methods. Berlin: Springer-Verlag. pp. 109–137.

Kunkel, J. G. & M. J. Jercinovic. 2012. Carbonate apatite formulation in cuticle structure adds resistance to microbial attack for American lobster. *Mar. Biol. Res*. (in press).

Kunkel, J. G., M. J. Jercinovic, D. A. Callaham, R. Smolowitz & M. Tlusty. 2005b. Electron microprobe measurement of mineralization of American lobster, *Homarus americanus*, cuticle: proof of concept. In: M. F. Tlusty, H. O. Halvorson, R. Smolowitz & U. Sharma, eds., Lobster Shell Disease Workshop. Aquatic Forum Series. Boston, MA: New England Aquarium. pp. 76–82.

Kunkel, J. G., L.- Y. Lin, Y. Xu, A. M. M. Prado, J. A. Feijó, P. P. Hwang & P. K. Hepler. 2001. The strategic use of good buffers to measure proton gradients about growing pollen tubes. In: A. Geitman, editor. Cell biology of plant and fungal tip growth. Amsterdam: IOS Press. pp. 81–94.

Laufer, H., M. Chen, M. Johnson, N. Demir & J. M. Bobbitt. 2012. The effect of alkylphenols on lobster shell hardening. *J. Shellfish Res*. 31:555–562.

Lawrence, P. A. 1966. Development and determination of hairs and bristles in the milkweed bug, *Oncopeltus fasciatus* (Lygaeidae, Hemiptera). *J. Cell Sci*. 1:475–498.

Locke, M. 2001. The Wigglesworth lecture: insects for studying fundamental problems in biology. *J. Insect Physiol*. 47:495–507.

Lowenstam, H. A. 1981. Minerals formed by organisms. *Science* 211: 1126–1131.

Marin, F. & G. Luquet. 2004. Molluscan shell proteins. *C. R. Palevol* 3:469–492.

Martin, J. W., K. A. Crandall & D. L. Felder. 2009. Preface. In: J. W. Martin, K. A. Crandall & D. L. Felder, editors. Decapod crustacean phylogenetics. London: CRC Press. pp. viii–xi.

Merritt, D. J. 2007. The organule concept of insect sense organs: sensory transduction and organule evolution. *Adv. Insect Physiol*. 33:192–241.

Mirtchi, A. A., J. Lemaître & E. Munting. 1991. Calcium phosphate cements: effect of fluorides on the setting and hardening of beta-tricalcium phosphate-dicalcium phosphate-calcite cements. *Biomaterials* 12:505–510.

Nikolov, S., M. Petrov, L. Lymperakis, M. Friák, C. Sachs, H.- O. Fabritius, D. Raabe & J. Neugebauer. 2010. Revealing the design principles of high-performance biological composites using *ab initio* and multiscale simulations: the example of lobster cuticle. *Adv. Mater. (Deerfield Beach Fla.)* 22:519–526.

Orr, J. C., V. J. Fabry, O. Aumont, L. Bopp, S. C. Doney, R. A. Feely, A. Gnanadesikan, N. Gruber, A. Ishida, F. Joos, R. M. Key, K. Lindsay, E. Maier-Reimer, R. Matear, P. Monfray, A. Mouchet, R. G. Najjar, G.-K. Plattner, K. B. Rodgers, C. L. Sabine, J. L. Sarmiento, R. Schlitzer, R. D. Slater, I. J. Totterdell, M.-F. Weirig, Y. Yamanaka & A. Yool. 2005. Anthropogenic ocean acidification over the twenty-first century and its impact on calcifying organisms. *Nature* 437:681–686.

Palmer, C. L., R. K. Horst & R. W. Langhans. 1997. Use of bicarbonates to inhibit *in vitro* colony growth of *Botrytis cinerea*. *Plant Dis*. 81:1432–1438.

Pohl, P., S. M. Saparov & Y. N. Antonenko. 1998. The size of the unstirred layer as a function of the solute diffusion coefficient. *Biophys. J*. 75:1403–1409.

Pouget, E. M., P. H. Bomans, J. A. Goos, P. M. Frederik, G. de With & N. A. Sommerdijk. 2009. The initial stages of template-controlled $CaCO_3$ formation revealed by Cryo-TEM. *Science* 323:1455–1458.

R Development Core Team. 2011. R: a language and environment for statistical computing. Vienna, Austria: R Foundation for Statistical Computing. http://www.R-project.org/.

Raabe, D., C. Sachs & P. Romano. 2005. The crustacean exoskeleton as an example of a structurally and mechanically graded biological nanocomposite material. *Acta Mater*. 53:4281–4292.

Richards, A. G. 1951. The integument of arthropods. St. Paul: University of Minnesota Press. 411 pp.

Ridgwell, A. & D. N. Schmidt. 2010. Past constraints on the vulnerability of marine calcifiers to massive carbon dioxide release. *Nat. Geosci.* 3:196–200.

Ries, J. B., A. L. Cohen & D. C. McCorkle. 2009. Marine calcifiers exhibit mixed responses to CO_2-induced ocean acidification. *Geol. Soc. Am.* 37:1131–1134.

Roer, R. D. & R. M. Dillaman. 1984. The structure and calcification of the crustacean cuticle. *Am. Zool.* 24:893–909.

Rosa, R. D. & M. A. Barracco. 2010. Antimicrobial peptides in crustaceans. *Invert. Surviv. J.* 7:262–284.

Santos, M. & P. F. Gonzalez-Diaz. 1977. A model for B carbonate apatite. *Inorg. Chem.* 16:2131–2134.

Seidl, B., K. Huemer, F. Neues, S. Hild, M. Epple & A. Ziegler. 2011. Ultrastructure and mineral distribution in the tergite cuticle of the beach isopod *Tylos europaeus* Arcangeli, 1938. *J. Struct. Biol.* 174:512–526.

Smolowitz, R. M., R. A. Bullis & D. A. Abt. 1992. Pathologic cuticular changes of winter impoundment shell disease preceding and during intermolt in the American lobster, *Homarus americanus*. *Biol. Bull.* 183:99–112.

Tao, J., D. Zhou, Z. Zhang, X. Xu & R. Tang. 2009. Magnesium-aspartate-based crystallization switch inspired from shell molt of crustacean. *Proc. Natl. Acad. Sci. USA* 106:22096–22101.

Tlusty, M. F., R. M. Smolowitz, H. O. Halvorson & S. E. DeVito. 2007. Host susceptibility hypothesis for shell disease in American lobsters. *J. Aquat. Anim. Health* 19:215–225.

Turley, C. M., J. M. Roberts & J. M. Guinotte. 2007. Corals in deep-water: will the unseen hand of ocean acidification destroy cold-water ecosystems? *Coral Reefs* 26:445–448.

Vega, F. J., V. M. Dávila-Alcocer & H. F. Filkorn. 2005. Characterization of cuticle structure in Late Cretaceous and Early Tertiary decapod Crustacea from Mexico. *Bull. Mizunami Fossil Museum* 32:37–43.

Waddy, S. L., D. E. Aiken & D. P. V. deKleijn. 1995. Control of growth and reproduction. In: J. R. Factor, editor. Biology of the lobster *Homarus americanus*. New York: Academic Press. pp. 217–266.

Wheatly, M. G. 1999. Calcium homeostasis in Crustacea: the evolving role of branchial, renal, digestive and hypodermal epithelia. *J. Exp. Zool.* 283:620–640.

Willis, J. H. 1999. Cuticular proteins in insects and crustaceans. *Am. Zool.* 39:600–609.

Wopenka, B. & J. D. Pasteris. 2005. A mineralogical perspective on the apatite in bone. *Mater. Sci. Eng. C* 25:131–143.

Wu, J., W. Sunda, E. A. Boyle & D. M. Karl. 2000. Phosphate depletion in the western North Atlantic Ocean. *Science* 289:759–762.

Zubkov, M. V., I. Mary, E. M. S. Woodward, P. E. Warwick & B. M. Fuchs. 2007. Microbial control of phosphate in the nutrient-depleted North Atlantic subtropical gyre. *Environ. Microbiol.* 9:2079–2089.